*34th EPS Conference on Plasma Phys. Warsaw, 2 - 6 July 2007 ECA Vol.**31F**, P-2.126 (2007)*

Heat pulse propagation studies around magnetic islands in TEXTOR

G.W. Spakman[1], G.M.D. Hogeweij[1], F.C. Schüller[1], I.G.J. Classen[1], C. Domier[4], A.J.H. Donné[1], R.J.E. Jaspers[1], M.Yu. Kantor[1,3], A. Krämer-Flecken[2], Y. Liang[2], E. Westerhof[1], J.W. Oosterbeek[1], M.J. van de Pol[1], E. Uzgel[2], H.K. Park[5], the TEXTOR-team

[1]FOM-Institute for Plasma Physics Rijnhuizen, Ass. EURATOM-FOM,*
PO Box 1207, 3430 BE Nieuwegein, The Netherlands, www.rijnhuizen.nl
[2] Institut für Energieforschung-Plasmaphysik, Forschungszentrum Jülich,
Ass. EURATOM- FZ Jülich, D-52425 Jülich, Germany*
[3] Ioffe Institute, RAS, Saint Petersburg 194021, Russia
[4] Dept. of Applied Physics, UC Davis, USA.
[5]Princeton Plasma Physics Laboratory, Princeton, New Jersey, U.S.A
**Partner in the Trilateral Euregio Cluster*

1. Introduction

The formation of magnetic islands in fusion machines is often observed to degrade confinement. Due to the fact that heat transport parallel to the toroidal magnetic field is much larger than perpendicular to the magnetic field, heat is expected to flow from the centre along the separatrix across the X-point to the plasma edge. Reduced flow of heat is expected through the magnetic island O-point. Whether the temperature profile in the vicinity of the O-point becomes flattened or not depends on the ratio of parallel to perpendicular transport, the island width and the power balance at the O-point. Heat transport inside the magnetic island is normally difficult to measure because of shallow temperature gradients inside the island. To measure heat transport in the flat temperature region of islands, perturbative transport techniques can be employed such as reported from LHD where: a) reduced transport at the 1/1 magnetic island O-point has been observed from the propagation of a cold pulse perturbation [1], and b) heat pulse propagation across a rational surface has revealed a local maximal phase delay which is due to the presence of a 2/1 magnetic island [2]. In tokamaks, perturbative transport experiments in the presence of islands are complicated by the spontaneous rotation of the islands with respect to the measurement frame. In the TEXTOR tokamak (R/a=1.75m/0.47m) large (w/a=0.25) statically locked m/n = 2/1 islands can easily be created by the application of the external perturbation field of the Dynamic Ergodic Divertor [3]. Furthermore a high power ECRH system [4] allows the creation of localized temperature perturbations which can be measured at the island's position with a high resolution 2D ECE-Imaging system [5]. With these tools a careful mapping of the heat transport around island has been made.

2. Experimental Setup and Data Analysis

To study the propagation of heat from centre to edge across the q=2 surface, the electron temperature is periodically modulated at 40 or 80 Hz at the high field side during an interval of 1s with a 140 GHz, 800 kW gyrotron [4], both inside and at the q=2 surface. The propagation of the modulation is measured with several ECE-diagnostics and SXR-cameras. Locally at the island radius at the low field side a high resolution 2D ECE-Imaging diagnostic (ECEI) consisting of 16(vertical) x 8(radial) channels covering an area of 17cm x 10cm [5], measures the propagation of the perturbation in detail. The radial observation area of ECE-I is varied from shot to shot to cover a radial region near the island O-and X-points by tuning the frequency of the local oscillator (BWO). The ECE-systems are cross-calibrated with Thomson Scattering. Inside the island at the low field side the optical thickness $\tau > 2.5$ such that the second harmonic X-mode ECE signals are proportional to the temperature. The SXR system covers both O-and X-point at the same time with 2 cameras. By reversing both the toroidal field and current the m/n = 2/1 island is poloidally rotated by 90 deg. which corresponds to a toroidal plasma shift of 180 deg. as observed by both the ECEI and SXR systems. In this way regions near both O-and X-point can be covered by ECE-I although in separate, but very reproducible, discharges. The phase delay with respect to the modulated source and amplitude of the oscillations are determined

for the first harmonic of the modulation by Fast Fourier Transforms. The experiments are performed at a toroidal field of 2.3 T, current 320 kA and line averaged density of $2 \cdot 10^{19}$ m^{-3}.

3. Experimental Results

A typical example of the ECEI results of the heat pulse propagation studies is shown in Fig. 1. For these experiments, the temperature was modulated by ECRH deposited with a width of 2cm at a radius of R=1.96m at the high field side, corresponding to ρ=0.37, which is inside the q=2 surface, located around ρ=0.57. For this specific case the modulation frequency of 40 Hz is well separated from other oscillations in the plasma (note that no sawteeth are present in these discharges with islands). A radial scan near O- and X-point by changing the ECE-I observation area in six reproducible discharges was performed (three for the O-point and three for the X-point), allowing to construct the ECE signals in the region from R=1.9–2.2m, (ρ=[0.23-1.0]), as shown in Fig. 1. For every discharge a single radial row of ECE-Imaging is plotted. A small discontinuity for overlapping areas measured at different discharges results due to minor cross calibration errors. Some channels especially near the edge are affected by suprathermal ECE radiation and are left out of the plot. For a reference discharge without island, data obtained from a 1D ECE-system is also plotted. Plotted are the average electron temperatures over the heat pulses, the phase difference with respect to the applied heat pulse and the amplitude of the heat pulse.

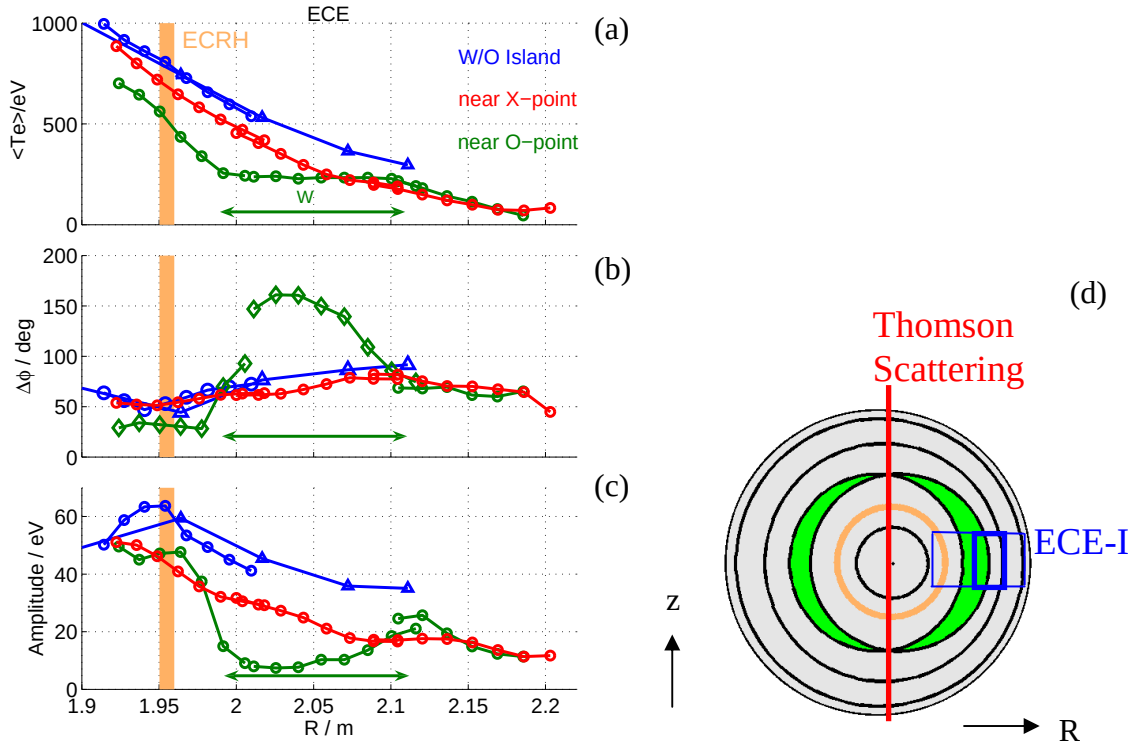

Figure 1, Scan near O- and X-point by ECE-Imaging at 40 Hz modulation frequency compared with a discharge without island. A single radial row of ECE-I (circles) is plotted for each discharge. For the reference discharge data from a 1D ECE-system has been plotted (triangles). The orange bar indicates the ECRH-deposition and the green arrow the island width a.) Average Temperature during modulation, b.) Phase delay first harmonic c.) Amplitude of the first harmonic d.) Schematic overview of the m/n=2/1 island position (green), ECRH-deposition radius (orange) and the ECE-Imaging observation area (thick blue lines) and the radius over which it is scanned in reproducible discharges (thin blue lines).

The first observation to make is that near the O-point the average temperature profile becomes flattened over a width w~11 cm. This is interpreted as the island width. Viewing the profile near the X-point indeed does not show a significant flat region. Note that the temperature at R< 1.98 m, i.e. at the hot outside of the island, is higher at the poloidal angle of the X-point than that of the O-point. This is due to the elliptical deformation of the non-rational flux surfaces by the large island [7].

The information on heat transport becomes apparent in the plot of the phase and amplitude of the heat pulses. Turning our attention first to the phase plot, it is seen that for plasmas without tearing modes the phase delay (proportional to the time delay) increases monotonically with the distance from the ECRH deposition surface. As soon as islands are excited, this picture changes drastically: the phase delay acquires a local maximum at the position where the island O-point is expected from the flattened average temperature profile. This shows that the heat-pulses are slowly propagating from the separatrix towards the island centre. The gradient in the phase delay near the X-point is almost flat compared to that near the O-point. This feature represents a large radial transport in this region. Near the plasma edge the phase delays and amplitudes of the measurements for both O- and X-point, nearly coincide again but at some lower level than for the reference discharge. This indicates that the overall transport is enhanced due to the presence of islands.
From the SXR measurements qualitatively similar observations have been made: a local maximum in the phase delay near the island O-point and flattened phase-delay near the island X-point.
The width of the island can be determined from both the width of the phase delay peak around the O-point crossing the nearly flat phase delay profile near the X-point. The width w~11cm and radial position correspond very well to that of the flattened part of the temperature profile.
The amplitude of the perturbations is smaller for discharges with islands than for the reference discharge as the overall confinement is poorer. The amplitude acquires a local minimum near the island O-point whereas the amplitude profile near the X-point is almost flat. This observation confirms that the heat is mainly lost through X-point

4. Observation of 2D Heat transport near the X-point

The 2D capability of the ECE-I system has been exploited for these investigations. In Fig. 2 a 2D image of the phase delay of a tip of the island close to the X-point is shown. The image is composed of three images from different radial positions obtained in the same discharges as shown in Fig. 1. The bottom row denoted by the red arrow is also shown in Fig. 1. In the radial direction a local maximum in the phase delay is observed. Just beyond the maximum a white line is plotted representing a calculated flux surface (for the situation without island). A dashed white line connecting points of equal phase delays converges to the solid white line close to the bottom. A complete vanishing of the maximum as expected for the X-point is not observed but might be below the observation area. It has to be noted that ECE-channels close to the low-field side edge (beyond the solid white line) are affected by suprathermal ECE-radiation which possibly decrease the phase delay, making the vanishing of the maximum due to X-point indistinct.

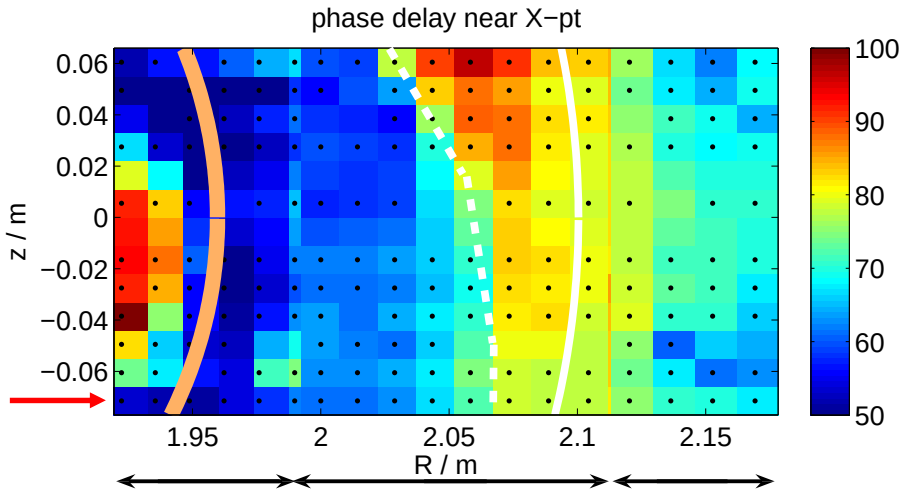

Figure 2, Observation of 2D heat pulse propagation near the X-point with ECE-I. The picture is composed of three images obtained from three discharges in which the Radial observation area was shifted (black arrows at the bottom indicate the three constituting images). The red arrow denotes the row which is shown in Fig. 1. The black dots denote the channels of ECE-Imaging that are evaluated. Cells without dots are interpolated. The orange line is the ECRH deposition radius determined from an equilibrium calculation without island. Solid white line is a calculated flux surface (without island) just beyond the maximum in the phase delay. The dashed white line connects points with nearly equal phase.

5. Derivation of transport coefficients

To compare the transport levels inside and outside the island, incremental electron heat diffusion coefficients can now be derived from the data shown in Fig. 1. In general, low heat diffusion coefficients lead to large gradients in the phase delay and amplitude profiles and conversely low gradients arise due to large transport coefficients. At large radii a slab geometry is a valid approximation. With negligible damping and convection the following relations hold for the heat diffusivity coefficients: $\chi_\phi = 3\omega/4\phi'^2 = \chi_A = 3\omega/4(A'/A)^2$, where (A'/A) is the relative gradient in the amplitude profile, ω the modulation frequency and ϕ' is the gradient in the phase delay. Corrections for geometrical effects [6] could be made, but for the situation under investigation here (large elongated islands and off-axis pulses) such corrections are only important very close to the island centre. The gradient in the phase is determined more accurately than the gradient in the amplitude. This method yields a heat diffusivity inside the island $\chi_\phi = 0.3$ m^2/s assuming constant χ inside the island and ϕ' taken the difference between O- and X-point over half the island width. Without island the island the heat diffusivity near the q=2 surface is $\chi_\phi = 2.5$ m^2/s.

6. Conclusion

The results shown here resemble the data from LHD [1] quite well: reduced transport inside the magnetic island O-point by one order of magnitude compared to the no-island case is observed. On the other hand, results of power balance calculations done for strong ECRH inside the island at TEXTOR [7], led to the conclusion that the heat diffusivity inside the island is similar to that of the bulk plasma, typically $\chi^{pb} = 1$m^2/s. The difference in both cases might be attributed to the difference in heat flux through the island: In the case of strong heating inside the island a temperature gradient builds up. On tokamaks it has been observed that above a critical T_e-gradient-length the heat diffusivity increases [8], so-called stiff profiles. It might be that the situation described in [7] was above this threshold, whereas the situation of low temperature gradients described here is below. Follow-up experiments with different temperature gradients inside islands could elucidate this difference.

Further, as expected, it was observed that the presence of the island strongly increases the radial heat transport in the plasma and that this transport is mainly channelled through the X-point. The heat transport along the field lines is thus dominating the overall transport properties in these cases with islands.

Acknowledgement

This work, supported by the European Communities under the Contract of Association between EURATOM-FOM, was carried out within the framework of the European Fusion Programme. The views and opinions expressed herein do not necessarily reflect those of the European Commission.

References

[1] S. Inagaki et al., Phys. Rev. Lett. **92** (2004), 055002
[2] M. Yakovlev et al., Phys. Plasmas **12** (2006), 092506
[3] H.R. Koslowski, et al., Plasma Phys. Control. Fusion **48** (2006), B53-B61
[4] E. Westerhof et al., Fusion Sci. Techn. **47** (2005), 108
[5] C.W. Domier et al., Rev. Sci. Instrum. **77** (2006), 10E924
[6] A. Jacchia et al., Phys. Fluids B **3** (1991), 3033
[7] I.G.J. Classen et al., Phys. Rev. Lett. **98** (2007)**,** 035001
[8] F. Ryter et al., Nucl. Fusion **43** (2003), 1396